

## Position Control of a DC Motor under Different Loads Using SMC and PID Control Methods

TAYFUN ABUT

Muş Department of Mechanical Engineering  
Mus Alparslan University, Mus, Turkey

### Abstract

*Various methods are proposed and applied for the control of Direct current (DC) motors used in many systems from past to present. These motors are operated under various loads in real life and loads cause a decrease in the running performance of the motor. In this study, modeling of dc motor and position control under different loads were performed using Sliding Mode Control (SMC) and Proportional-Integral-Derivative (PID) control methods. Also, the position results of the motor were evaluated using the Mean-Square-Error (ISE) performance criterion. The obtained results were given in the form of graphics and tables and analyzed.*

**Keywords:** Modeling; Sliding Mode Control(SMC); Proportional-Integral-Derivative(PID); Different Loads

### 1. INTRODUCTION

Cost, ease of control, long life and silent operation, etc. Direct current (DC) motors have been used frequently from past to present due to their characteristics. Since these motors have a wide area of use in the literature, control studies have been actively researched and continue to be investigated. Ohishi et al. He worked on microprocessor-controlled DC motor control for non-load sensitive position servo system [1]. Weerasooriya and El-Sharkawi worked on the identification and control of a DC motor using neural networks using a backpropagation algorithm [2]. Baek and Kuc proposed the control of DC motors with

adaptive PID learning [3]. Mehta and Chiasson [4] have done theory and experimental work on the nonlinear control of a series of DC motors. Tang realized the speed and position control of real-time DC motor by using a PID control method with TMS320C31 DSK with on-line parameter setting [5]. Ruderman et al. optimum control of the DC motor has been realized in the state space [6]. Position control of the DC motor was carried out by using Thomas and Poongodi genetic algorithm based PID controller [7]. Adhikari et al. realized the control of the DC motor using the PID control method. They found the control coefficients of the method by using the Ziegler Nichols and the genetic algorithm [8].

Anandaraju et al. He has performed the speed control of a DC motor by obtaining the control coefficients of the PID method with a genetic algorithm [9]. Yousef carried out the experimental setup and verification of servo DC motor position control based on the integral sliding mode control approach [10]. Wang and Suh performed precise synchronous speed and position tracking of brushed dc motors using nonlinear time-frequency control [11]. In another study, the Kalman filter was used to estimate DC motor speed and both PID and LQR controllers were used to control the motor [12]. Chaudhary et al. ANFIS based speed control of DC motor. It has been recommended and implemented [13]. Khubalkar et al. modeled and controlled permanent magnet brushless DC motor drive using a fractional proportional-integral-derivative controller [14]. Qader made a study to determine the most appropriate controller strategy for DC motors [15]. Usman et al. performed an estimation of permanent magnet DC motor parameters via universal adaptive stabilization [16]. DC motors are operated under various loads in real life and loads cause a decrease in the running performance of the motor. In this study, the modeling of DC motor and position control under different loads were performed using Sliding Mode Control (SMC) and Proportional-Integral-Derivative (PID) control methods. Also, the angular position results of the motor were evaluated using the Mean-Square-Error (MSE) performance criterion. The obtained results were given in the form of graphics and tables and analyzed.

## 2. MATHEMATICAL MODEL OF DC MOTOR

Direct current (DC) motors are widely used in a variety of industrial and electronic equipment where high accuracy position control is required. The model of the dc motor is given in the equations below. Figure 1 shows the direct current (DC) motor.

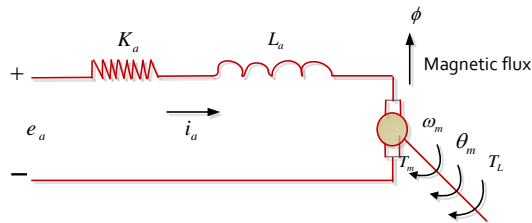


Fig.1. Direct current (DC) motor model

The moment received from the electric motor;

$$T_m(t) = K_m \cdot \Phi \cdot i_a(t) = K_i \cdot i_a(t) \quad (1)$$

$$\frac{di_a}{dt} = \frac{1}{L_a} \cdot e_a - \frac{R_a}{L_a} \cdot i_a - \frac{1}{L_a} \cdot e_b \quad (2)$$

$$T_m = K_i \cdot I_a \quad (3)$$

$$e_b = K_b \cdot \frac{d\theta_m}{dt} = K_b \cdot \omega_m(t) \quad (4)$$

$$J_m \frac{d^2\theta_m}{dt^2} = T_m - T_L - B_m \cdot \frac{d\theta_m}{dt} \quad (5)$$

If we take our variables as  $i_a$ ,  $\theta_m$  and  $\omega_m$ , the equations of state from the first order can be written as follows.

$$\dot{x} = Ax + Bu \quad (6)$$

$$\begin{bmatrix} \frac{di_a}{dt} \\ \frac{d\omega_m}{dt} \\ \frac{d\theta_m}{dt} \end{bmatrix} = \begin{bmatrix} -\frac{R_a}{L_a} & -\frac{K_b}{L_a} & 0 \\ \frac{K_i}{J_m} & -\frac{B_m}{J_m} & 0 \\ 0 & 1 & 0 \end{bmatrix} \begin{bmatrix} i_a \\ \omega_m \\ \theta_m \end{bmatrix} + \begin{bmatrix} \frac{1}{L_a} \\ 0 \\ 0 \end{bmatrix} \cdot e_a - \begin{bmatrix} 0 \\ \frac{1}{J_m} \\ 0 \end{bmatrix} \cdot T_L(t) \quad (7)$$

$$\frac{\theta_m(s)}{E_a(s)} = \frac{\theta_m(s)}{E_a(s)} = \frac{K_i}{L_a J_m s^3 + (R_a J_m + B_m L_a) s^2 + (K_b K_i + R_a B_m) s} \quad (8)$$

The parameters of the dc motor are shown in Table 1.

**Table 1. Parameters of Dc motor**

<i>Symbol</i>	<i>Description</i>	<i>Units</i>	<i>Value</i>
<i>m</i>	Body Mass	<i>kg</i>	10
<i>J</i>	Body Inertia	<i>kgm<sup>2</sup></i>	0.171
<i>K<sub>m</sub></i>	Motor Constant	<i>Nm/A</i>	3520
<i>R<sub>a</sub></i>	Motor Resistance	<i>Ohm</i>	55
<i>l<sub>o</sub></i>	Leg Length	<i>m</i>	0.323
<i>L<sub>m</sub></i>	Motor electric inductance	<i>H</i>	0.3
<i>B<sub>m</sub></i>	The damping ratio of the system friction constant	<i>Nm.</i>	0.097

### 3. CONTROLLER DESIGN

Using two different control methods under different loads, a controller has been designed to reach the desired position of the DC motor and obtain the minimum error in position control. It is aimed here that  $\theta$  (actual motor angle) follows  $\theta_d$  (desired motor angle) with minimum error. DC motor was controlled under different loads using PID and Sliding Mode Control (SMC) control methods.

#### 3.1. PROPORTIONAL-INTEGRAL DERIVATIVE (PID) CONTROL

The Proportional-Integral-Derivative (PID) control method is a method used in many applications. The basic mathematical equation of the PID control method is given in equation 9 [17]. Ziegler-Nichols method was used to find the PID control coefficients and closed-loop control type was used in this method [18].  $\theta_d$  Reference input angle signal,  $\theta$  the output angle of the real system,  $e = \theta_d - \theta$  error signal,  $K_p$  proportional gain,  $K_i$  integral gain, and  $K_d$  derivative gain.

$$u(t) = K_p e(t) + K_i \int_0^t e(t) dt + K_d \frac{d}{dt} e(t) \quad (9)$$

#### 3.2. SLIDING MODE CONTROL (SMC) METHOD

Sliding mode control is a special case of variable structured control. SMC is a special form of variable structured control. This method initially forces state variables to go on the sliding surface and then, they are kept on such surface and afterward, are shifted towards the origin

[19]. Therefore, it is called the sliding surface as well as the switching surface. Due to the nature of this method, it has a non-continuous control structure. This discontinuous check mark causes chattering. This harms the physical system elements. One of the ways to prevent this is to replace the discontinuous signum function in the sliding mode control with the saturation function, which is a continuous approximation of this function [20-21]. The angular position of the motor is the control variable. The block diagram of the sliding mode control (SMC) method is given in Figure 2. Equations containing the error and its derivative are given in equations 10 and 11.

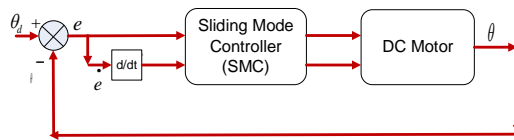


**Fig.2. The control structure of the SMC method.**

$$e(t) = \theta_d(t) - \theta(t) \tag{10}$$

$$\dot{e} = \dot{\theta}_d - \dot{\theta} \tag{11}$$

In the expressions given in the equations given above,  $\theta_d$  the reference input angle signal  $\theta$  is called the output angle of the real system,  $e$  and  $\dot{e}$  the error signal respectively. The sliding surface ( $s$ ) is given in equations 12 and 13.  $\lambda$  is a positively defined symmetric matrix and  $k$  is a constant parameter. Signum is the sign function and  $s$  functions as switching. The Lyapunov criterion was used for the stability of the system. The saturation function is used to solve the cracking problem.  $\phi$  shows the thickness of the boundary layer.

$$s = \dot{e} - \lambda e \tag{12}$$

$$\dot{s} = \ddot{e} - \lambda \dot{e} \tag{13}$$

$$u = -k * \text{sign}(s) \tag{14}$$

$$\text{sat} (s / \phi) = \begin{cases} \frac{s}{\phi} & \text{if } \left| \frac{s}{\phi} \right| \leq 1 \\ \text{sgn}(s / \phi) & \text{if } \left| \frac{s}{\phi} \right| > 1 \end{cases} \tag{15}$$

#### 4. SIMULATION RESULTS

In this section, simulation studies obtained by using mathematical model equations of dc motor are given. PID and sliding mode control algorithms are used in the control of the DC motor. The control variable is the motor angular position. A fixed value and sine wave input are applied to the motor model. Also, the motor was controlled under 10, 100, and 1000 N load, respectively, without load. The results of the control methods recommended under different loads were obtained according to the performance criteria (Mean Square Error (MSE)) and the methods were examined. The simulation time was set as 10 seconds. Figure 3 shows a constant value of the motor without load and the angular motor position and error graph obtained by using the PID control method. Figure 4 shows a constant value of the motor under 10 N load and the angular motor position and error graph obtained by using the PID control method. Figure 5 shows a fixed value of the motor under 100 N load and angular motor position and error graph obtained by using the PID control method.

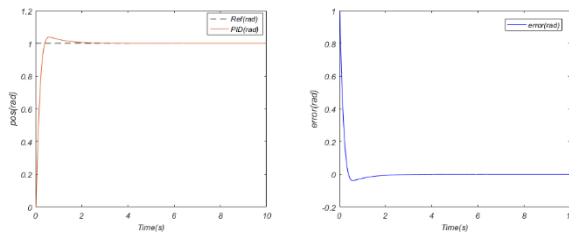


**Fig.3. The angular position and error graph obtained by applying a constant input and PID control method (load TL = 0 N)**

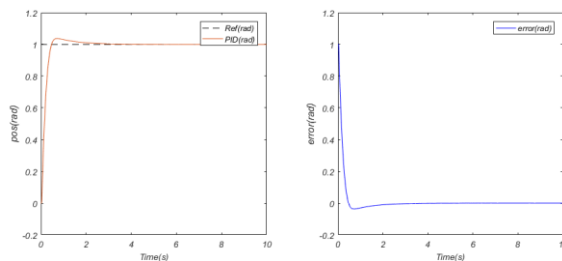


**Fig. 4. The angular position and error graph obtained by applying a constant input and PID control method (load TL = 10 N)**

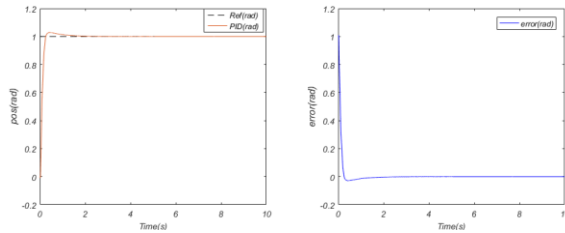


**Fig. 5. The angular position and error graph obtained by applying a constant input and PID control method (load TL = 100 N)**

In Figure 3, it was seen that the maximum overshoot occurred in the graph obtained as a result of using the PID control method against a constant input value of the motor with no load. Looking at the angular motor error graph, it was seen that the motor reached the settling time in about 7 seconds. In Figure 4, it was seen that the maximum overshoot occurred in the graph obtained as a result of the use of the PID control method against a constant input value of the motor under 10 N load. Looking at the angular motor error graph, it was seen that the motor reached settling time in about 5 seconds. In Figure 5, it is seen that the maximum overshoot occurs but the amplitude decreases in the graph obtained as a result of using the PID control method against a constant input value of the motor under 100 N load. Looking at the angular motor error graph, the motor's 2.2. It was observed that it reached the settlement time per second. In Figure 6, the angular motor position and error graph obtained by using a fixed input and SMC control method of the motor without load is given. Figure 7 shows the angular motor position and error graph obtained by using a fixed input and SMC control method of the motor under 10 N load. Figure 8 shows the angular motor position and error graph obtained by using a fixed input and SMC control method of the motor under 100 N load.

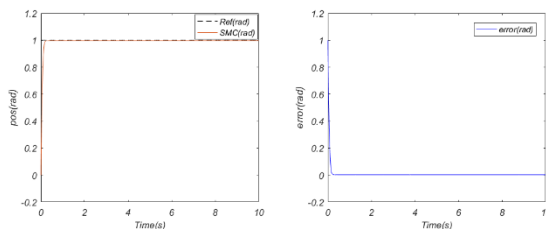


**Fig.6. The angular position and error graph obtained by applying a constant input and SMC control method (load TL = 0 N)**

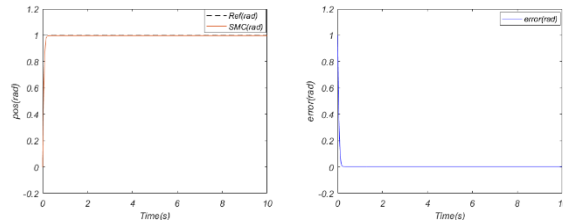


**Fig. 7. The angular position and error graph obtained by applying a constant input and SMC control method (load TL = 10 N)**

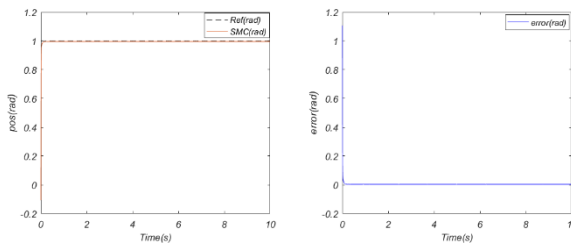


**Fig.8. The angular position and error graph obtained by applying a constant input and SMC control method (load TL = 100 N)**

In Figure 6, it is seen that maximum overshoot does not occur in the graph obtained as a result of using the SMC control method against a fixed input value of the motor without load. Looking at the angular motor error graph, the motor is about 0.3. It was observed that it reached the settlement time per second. In Figure 7, it was seen that the maximum overshoot did not occur in the graph obtained as a result of using the SMC control method against a fixed input value of the motor under 10 N load. Looking at the angular motor error graph, the motor is about 0.15. It was observed that it reached the settlement time per second. In Figure 8, it was seen that the maximum overshoot did not occur in the graph obtained as a result of using the SMC control method against a fixed input value of the motor under 100 N load. Looking at the angular motor error graph, the motor is about 0.01. It was observed that it reached the settlement time per second. Error results were obtained according to Mean Absolute Error (MSE) performance criteria in Table 1. The equation of the performance criterion for MSE is given below.

$$MSE = \frac{1}{N} \left( \sum_j^N y_{m_j} - y_{s_j} \right)^2 \tag{16}$$

$y_{aj}$  robot requested  $j$ . If the value is  $y_j$ , the robot  $j$ . shows its true value.  $y$  represents the angular position ( $\theta$ ) of the motor.  $j = 1, 2, 3, 4, \dots, N$ . Table 1 shows the error results obtained by using the performance criteria of the PID and SMC control methods against a fixed input value, which is the MSE.

**Table 1. The error results according to performance criteria.**

MSE	PID Control	SMC
TL=0	0.0097	0.0030
TL=10	0.0118	0.0031
TL=100	0.0072	0.0007

According to the no-load angular position results of the motor given in Table 1, the best error rate for a fixed input value was obtained by the SMC control method and the result was 0.0030 radians. The value obtained using the PID control method is 0.0097 radians. When under 10 N load given in the table, the best error rate was again obtained by SMC control method and the result was 0.0118 radians. The value obtained using the PID control method is 0.0031 radians. The best error rate obtained under 100 N load, another load value given in the table, was also obtained by the SMC control method and the result was 0.0072 radians. The value obtained using the PID control method is 0.0007 radians. Considering the results obtained, it is seen that the best error rate is obtained with the SMC method. In general, it is seen that the SMC method shows superior performance.

## 5. DISCUSSION AND CONCLUSION

In this study, modeling of DC motor and angular position control was performed using Proportional-Integral-Derivative (PID) and Sliding Mode Control (SMC) control methods. The control performance of the system was evaluated using the MSE criteria. When the results obtained with the SMC method are observed, the best performance result has been obtained in terms of both maxima exceeding and settling time. The values obtained by using PID, another control method given in the table, did not give as good results as the SMC

method. Considering the results obtained, the lowest error rate was obtained using the SMC method under 100 N load and its value is 0.0007 radians. In general, it is seen that the SMC method shows superior performance. The method can be applied in a real-time laboratory environment in future studies.

## REFERENCES

1. Ohishi, K., Nakao, M., Ohnishi, K., and Miyachi, K. (1987). Microprocessor-controlled DC motor for load-insensitive position servo system. *IEEE Transactions on Industrial Electronics*, (1), 44-49.
2. Weerasooriya, S., and El-Sharkawi, M. A. (1991). Identification and control of a dc motor using back-propagation neural networks. *IEEE transactions on Energy Conversion*, 6(4), 663-669.
3. Baek, S. M., and Kuc, T. Y. (1997). An adaptive PID learning control of DC motors. In 1997 IEEE International Conference on Systems, Man, and Cybernetics. Computational Cybernetics and Simulation (Vol. 3, pp. 2877-2882). IEEE.
4. Mehta, S., and Chiasson, J. (1998). Nonlinear control of a series DC motor: theory and experiment. *IEEE Transactions on industrial electronics*, 45(1), 134-141.
5. Tang, J. (2001). PID controller using the TMS320C31 DSK with online parameter adjustment for real-time DC motor speed and position control. In ISIE 2001. 2001 IEEE International Symposium on Industrial Electronics Proceedings (Cat. No. 01TH8570) (Vol. 2, pp. 786-791). IEEE.
6. Ruderman, M., Krettek, J., Hoffmann, F., and Bertram, T. (2008). Optimal state space control of DC motor. *IFAC Proceedings Volumes*, 41(2), 5796-5801.
7. Thomas, N., and Poongodi, D. P. (2009, July). Position control of DC motor using genetic algorithm based PID controller. In *Proceedings of the world congress on engineering* (Vol. 2, pp. 1-3).
8. Adhikari, N. P., Choubey, M., and Singh, R. (2012). DC motor control using Ziegler Nichols and genetic algorithm technique. *International Journal of Electrical, Electronics and Computer Engineering*, 1(1), 33-36.
9. Anandaraju, M. B., Puttaswamy, P. S., and Singh Rajpurohit, J. (2011, July). Genetic algorithm: an approach to velocity control of an electric dc motor. In *IJCA* (Vol. 26, No. 1, pp. 37-43).
10. Yousef, A. (2011). Experimental set up verification of servo DC motor position control based on integral sliding mode approach. *JES. Journal of Engineering Sciences*, 39(5), 1095-1110.
11. Wang, X., and Suh, C. S. (2017). Precision concurrent speed and position tracking of brushed dc motors using nonlinear time-frequency control. *Journal of Vibration and Control*, 23(19), 3266-3291.
12. Abut, T. (2016). Modeling and Optimal Control of a DC Motor. *Int. J. Eng. Trends Technol*, 32(3), 146-150.

13. Chaudhary, H., Khatoun, S., and Singh, R. (2016, November). ANFIS based speed control of DC motor. In 2016 Second International Innovative Applications of Computational Intelligence on Power, Energy and Controls with their Impact on Humanity (CIPECH) (pp. 63-67). IEEE.
14. Khubalkar, S., Junghare, A., Aware, M., and Das, S. (2017). Modeling and control of a permanent-magnet brushless DC motor drive using a fractional order proportional-integral-derivative controller. *Turkish Journal of Electrical Engineering & Computer Sciences*, 25(5), 4223-4241.
15. Qader, M. R. (2019). Identifying the optimal controller strategy for DC motors. *Archives of Electrical Engineering*, 68(1).
16. Usman, H. M., Mukhopadhyay, S., and Rehman, H. (2019). Permanent magnet DC motor parameters estimation via universal adaptive stabilization. *Control Engineering Practice*, 90, 50-62.
17. Ziegler, J. G., and Nichols, N. B. (1942). Optimum settings for automatic controllers. *trans. ASME*, 64(11).
18. Abut, T. and Soyguder, S. (2018). Interface Design and Performance Analysis for a Haptic Robot. *Muş Alparslan Üniversitesi Fen Bilimleri Dergisi*, 6(2), 553-560.
19. Utkin, V. I. (1993). Sliding mode control design principles and applications to electric drives. *IEEE transactions on industrial electronics*, 40(1), 23-36.
20. Utkin, V., Guldner, J., and Shijun, M. (1999). *Sliding mode control in electro-mechanical systems* (Vol. 34). CRC press.
21. Abut, T., and Soygüder, S. (2018, May). Haptic industrial robot control and bilateral teleoperation by using a virtual visual interface. In *2018 26th Signal Processing and Communications Applications Conference (SIU)* (pp. 1-4). IEEE.

## APPENDIX

Nomenclature	
$i_a$	Motor current
$R_a$	Motor resistance
$e_b$	emf
$T_L$	Load torque
$\phi$	Magnetic flux
$J_m$	Moment of inertia
$B_m$	Viscous damping coefficient
$L_a$	Motor inductance
$e_a$	Motor voltage
$K_b$	emf constant
$\theta_m$	Angular rotation of the rotor
$K_i$	Torque constant
$w_m$	Angular velocity of the rotor